

Title: Quantifying changes in fish population stability using statistical early warnings of regime shifts

Authors: Jonathan A. Walter¹, Levi S. Lewis², James A. Hobbs², and Andrew L. Rypel^{1,2}

¹Center for Watershed Sciences, University of California, Davis, California, USA

²Department of Wildlife, Fish, and Conservation Biology, University of California, Davis, California, USA

Author emails:

JAW: jawalter@ucdavis.edu

LSL: lslewis@ucdavis.edu

JAH: jahobbs@ucdavis.edu

ALR: rypel@ucdavis.edu

Running head: Fish population early warnings

Key words: abrupt change, delta, estuary, fish, regime shift, river, stability

Open data and code: This research is based on publicly available data cited in the manuscript text. Derived data products are available via the Environmental Data Initiative repository: <https://doi.org/10.6073/pasta/aa552e1f82f95a33c2ea657e3c0706e4>. Derived data products and code reproducing these results are available on Zenodo: <https://doi.org/10.5281/zenodo.14907908>.

1 **Abstract**

2 Ecological conservation and management benefits from tools that can foresee impending
3 problems, or those in early stages. Statistical early warnings of regime shifts, which can identify
4 generic changes in system behavior associated with stability loss and potential abrupt changes to
5 a new, distinct state, are theoretically well grounded and have been successfully applied in
6 real-world settings. However, early warning indicators have seldom been applied to empirical
7 animal population data. We quantified early warning metrics in 29 fishes using > 4 decades of
8 monitoring data from the San Francisco Estuary and Sacramento-San Joaquin river system to
9 develop an index describing the magnitude of evidence of population stability loss and potential
10 regime shifts, relative to other studied species. Spatial synchrony increased in over twice as many
11 species as it decreased, but temporal variance and lag-1 autocorrelation showed no tendency to
12 have increased across species species. A composite early warning indicator (EWI) index
13 developed from these metrics identified higher-risk species (e.g., white croaker, tule perch) from
14 lower-risk ones (e.g., northern anchovy, fathead minnow). The composite index was uncorrelated
15 with long-term abundance trends or whether the species is native or non-native. We also
16 developed an index of confidence in the composite EWI score; considering both the EWI score
17 and confidence index simultaneously suggests possible responses for research and management.
18 For high EWI score, high confidence species may be candidates for targeted research and
19 interventions, while high EWI score, low confidence species may be candidates for enhanced
20 monitoring to better constrain population dynamics. Despite concerns about attributing changes
21 in EWI metrics to regime shifts in short time series, there appears to be value in applying generic
22 EWIs to population time series of animals with generation times ≥ 1 year, and approaches like
23 ours may be valuable when little is known about organism life history, and when applying a
24 consistent protocol can facilitate comparison across many species.

25 **Introduction**

26 Species conservation and ecosystem management are resource limited, motivating creative
27 ways to identify priorities for enhanced monitoring, management interventions, and scientific
28 study. Prioritization schemes that can foresee impending problems, or those in early stages, can
29 be especially valuable (Dietze et al., 2018; Scheffer et al., 2009), in part because interventions at
30 these incipient stages tend to be less costly and more effective (Ellis et al., 2011; Mandel et al.,
31 2010). Statistical early warnings of regime shifts quantify changes in the dynamics of a system
32 that are associated with abrupt changes between system states (Kéfi et al., 2014; Dakos et al.,
33 2008; Scheffer et al., 2009). Here, a regime shift is defined as an abrupt change to a new, distinct
34 state—such as a shift from a clear-water to an algal bloom state in a lake—which is assumed to
35 correspond to a shift from one dynamical basin of attraction to another. Early warning indicators
36 include measures of variance, autocorrelation, and other distributional properties (Scheffer et al.,
37 2009; Dakos et al., 2012; Kéfi et al., 2014; Seekell et al., 2011). Despite a robust body of theory
38 on early warning indicators (EWIs; e.g., Scheffer et al., 2009; Kéfi et al., 2014; Dakos et al.,
39 2012) and successful applications in anticipating regime shifts in real-world ecosystems (e.g.,
40 Pace et al., 2017; Wilkinson et al., 2018), EWIs have scarcely been applied to animal population
41 data to evaluate potential regime shifts in population dynamics.

42 Well-developed theory on the stability of complex systems and regime shifts proposes that
43 regime shifts may be preceded by general changes in system dynamics, including increased
44 variance and autocorrelation (Dakos et al., 2012; Kéfi et al., 2014; Buelo et al., 2018; Nolting and
45 Abbott, 2016; Patterson et al., 2021; Scheffer et al., 2009). The intuition behind these dynamical
46 changes is often illustrated using a so-called “ball and cup diagram” representing a system’s
47 stability landscape (see, e.g., Figure 1 of Scheffer et al., 2009). A ball representing the system
48 state sits in a depression in the stability landscape, representing an attractor. Modest perturbations
49 (e.g., environmental variation) nudge the ball away from its attractor, causing the ball’s position in
50 the stability landscape to vary. As the system’s stability erodes, an equivalent perturbation moves

51 the ball further from the attractor (i.e., increased variance). The ball also moves more slowly back
52 toward the attractor, causing measurements of the system at successive times to become more
53 similar to the previous one (i.e., increased autocorrelation). For spatially extended systems,
54 increases in spatial variance and autocorrelation may also accompany loss of resilience as a
55 regime shift is approached (Scheffer et al., 2009; Kéfi et al., 2014; Buelo et al., 2018). When a
56 regime shift takes place, some perturbation ‘kicks’ the ball into a different basin of attraction.
57 Empirical research in a range of settings has successfully applied EWIs to the prediction of
58 regime shifts, even developing functioning regime shift alarm systems (Carpenter et al., 2011;
59 Wilkinson et al., 2018) and demonstrating that early intervention triggered by an EWI-based
60 alarm system can reverse an ecosystem regime shift (Pace et al., 2017).

61 To date, natural populations of animals are largely unexplored from the perspective of EWIs,
62 and differences between animal populations and other applications of EWIs should make us
63 cautious. One important difference is that many successful applications of EWIs in real-world
64 systems feature much higher data density (e.g., hourly) on organisms like phytoplankton with
65 rapid growth and generation times. By contrast, populations of animals that have generation times
66 ≥ 1 year are often censused only once per year, and variation in higher-frequency (e.g., monthly)
67 measurements may likely confound demographic change with organism phenology or behavior.
68 As a result, it may take many decades to accumulate analogous data. With fewer observations and
69 lower sampling resolution, we might expect EWI metrics to have greater sampling variation, and
70 for shorter lags (in terms of number of observations) between changes in EWI metrics and a
71 regime shift. Despite this, many of the same statistics used as EWIs (e.g., measures of temporal
72 variance) are *also* ubiquitous metrics of stability in ecology (Donohue et al., 2016; Kéfi et al.,
73 2014; Wang and Loreau, 2014; Schindler et al., 2015). Thus, it stands to reason that there is value
74 to applying EWI metrics to animal population time series to investigate changes in population
75 stability, even if specific connections to regime shifts are imprecise. Additionally, while the field
76 has often been concerned about catastrophic regime shifts, EWIs can indicate more subtle

77 changes in regime (Kéfi et al., 2013); and while EWIs agnostic to the direction of change in the
78 focal variable, whether an increase or decrease in the focal variable is harmful is
79 context-dependent. For example, we may be concerned about population crashes (decreases) in
80 native species, but about population booms (increases) in non-native ones.

81 We quantified temporal change in regime shift early warning indicator statistics (EWIs) in a
82 suite of 31 fish species in central California, USA by leveraging long-term monitoring studies in
83 the San Francisco Bay Estuary and Sacramento-San Joaquin river system spanning more than
84 four decades. We developed a composite relative index of change in EWI/stability metrics and
85 asked whether values of this index were associated with long-term population trends or
86 native/non-native status. Additionally, we developed a confidence metric that takes into account
87 differences among species in data quality and agreement across spatial units and metrics.
88 Considering these two axes, composite EWI score and certainty, can facilitate prioritization of
89 research and management action. For example, studying or (if known) managing drivers of
90 population change could be logical steps for high EWI score/high confidence species, whereas
91 improving monitoring may be needed for high EWI score/low confidence taxa.

92 **Methods**

93 **Study system**

94 The San Francisco Estuary and Sacramento and San Joaquin river systems form a large
95 estuary and inland delta draining the Central Valley of California, USA. A region with a large
96 human population and intensive agriculture, the system's geomorphology, hydrology, and biota
97 are heavily altered by human activities. Dams and water diversions have altered the magnitude
98 and timing of downstream flows (Hanak, 2011; Yarnell et al., 2015), and water control structures
99 have restricted access to spawning and rearing habitats (Hanak, 2011; Moyle, 2002). Climate
100 warming and changes in flows have jointly altered water temperature (Brown et al., 2013; Willis
101 et al., 2021). Invasions of numerous aquatic organisms have altered habitat quality, primary
102 production, and trophic and competitive interactions (Moyle, 2002; Moyle et al., 2011). Several

103 fish populations, especially those of native anadromous fishes, are in steep decline (Moyle et al.,
104 2011), including including delta smelt, winter and spring run Chinook salmon (*Oncorhynchus*
105 *tshawytscha*) and southern distinct population segment green sturgeon (*Acipenser medirostris*),
106 each of which receive protections under state and federal Endangered Species Acts. Additionally,
107 longfin smelt (*Spirinchus thaleichthys*) has undergone major population declines (Tobias et al.,
108 2023) and is listed under the California and Federal Endangered Species Acts; and white sturgeon
109 (*A. transmontanus*) became a formal candidate for listing under the California Endangered
110 Species Act in 2024. These concerns and others have motivated multiple long-running,
111 multi-location monitoring studies that can be leveraged to study the dynamics of target and
112 non-target taxa (Stompe et al., 2020; Tempel et al., 2021; Colombano et al., 2022). However,
113 many fish species remain understudied, leading to uncertainties concerning their population
114 dynamics and responses to changing environmental conditions.

115 **Data**

116 We analyzed a suite of long-term fish monitoring data in Central California for potential early
117 warnings of regime shifts. (Bashevkin et al., 2024) compiled data from 10 monitoring studies; we
118 selected data from 3 studies (Table 1), focusing on those that have operated the longest and over
119 the broadest geography, and conducted sampling in fall months (September-December). We used
120 data spanning 1980 to 2023 because effort measures (e.g., sample volume) began becoming
121 widely available in the selected monitoring studies in 1980. We combined fall fish sampling with
122 determinations of age-0 maximum lengths thresholds based on expert knowledge and
123 length-frequency analyses (Walter et al. *in review*) to quantify fall age-0 fish catch per unit effort
124 (CPUE), except in cases where this was inconsistent with aspects of species life history, as
125 detailed here. For white sturgeon, we used a threshold of 1000 mm, corresponding to an age of
126 approximately 10 years; white sturgeon begin reaching reproductive maturity at $\approx 10 - 15$ years
127 of age (Blackburn et al., 2019).

128 We focused on fall age-0 CPUE for two primary reasons: 1) the sampling gears used in these

Monitoring study	First year	Months	Method	Regions sampled
SFBS	1980	All	Midwater trawl, otter trawl	Central, Confluence, San Pablo, South Bay, Suisun
DJFMP	1976	All	Beach seine, midwater trawl	Central, Confluence, North Delta, San Pablo Bay, South Delta, Suisun, Sacramento River, San Joaquin River
FMWT	1967	Sep-Dec	Midwater trawl	Central, Confluence, Napa River, North Delta, San Pablo Bay, South Delta, Suisun

Table 1: Attributes of monitoring studies contributing data to this study. SFBS = San Francisco Bay Study. DJFMP = Delta Juvenile Fish Monitoring Program. FMWT = Fall Midwater Trawl Survey.

129 monitoring programs primarily select for small-bodied fishes, so excluding larger size classes,
130 which are caught less reliably, reduces noise arising from sampling variation; 2) most studied
131 species spawn in spring to early summer and must persist through relatively poor (e.g., low flow,
132 supraoptimal water temperatures, low dissolved oxygen) conditions during summer and early fall
133 before the wet season begins—as a result, fall age-0 abundances provide an index of recruitment.
134 Point observations were aggregated by region-sampling method combinations and to an annual
135 time step by averaging. Some sampling methods (e.g., midwater trawl) are used by multiple
136 monitoring programs, with some differences in detailed sampling protocols, but preliminary
137 analyses and earlier research (Walter et al. *in review*) showed good agreement between samples
138 using the same method, but greater variability between methods. The different sampling methods

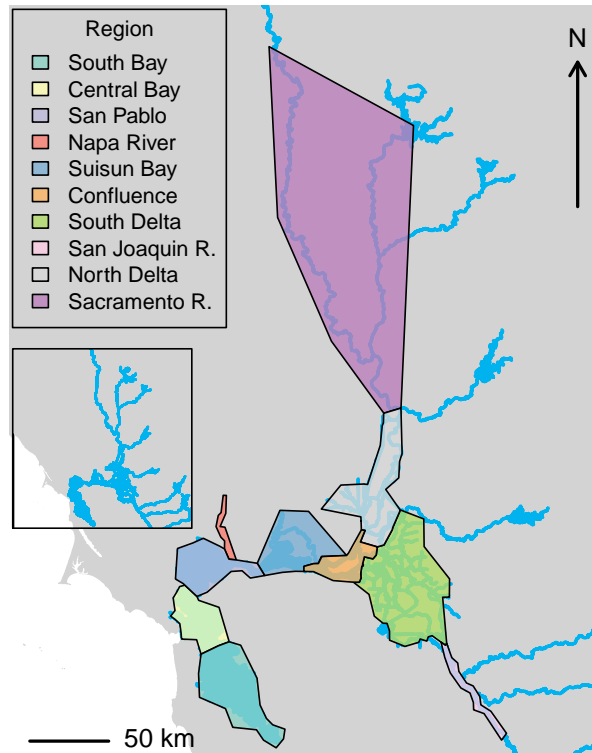


Figure 1: Map of study area and and analysis regions.

139 contributing to this study (midwater trawl, beach seine) sample different habitats (pelagic,
 140 benthic, and littoral, respectively), and monitoring locations span different regions with
 141 characteristic environmental conditions and fish communities (Figure 1) so we considered each
 142 region-sampling method combination a spatial unit. All fishing gears have selectivity biases
 143 related to fish size and portion of the water column sampled (Zale et al., 2012; Mitchell et al.,
 144 2017), making it difficult to simply combine catch information across surveys. We collated data
 145 on 39 candidate species, focusing on a subset of relatively commonly sampled and relatively
 146 abundant species, as well as those identified by wildlife and natural resource agency partners as
 147 species of interest, though some species were later discarded for having insufficient data for our
 148 analyses, resulting in a total of 29 species (Table S1).

149 **Analyses**

150 We focused on three early warning indicator (EWI) statistics: the temporal coefficient of
151 variation (CV), the lag-1 temporal autocorrelation, and spatial synchrony. The temporal CV and
152 lag-1 temporal autocorrelation were computed for each region-gear type combination in moving
153 temporal windows so that we could quantify temporal trends in each. The moving window width
154 was 5 years. As a robustness check, we also computed results using a window width of 7 years.
155 EWI statistics were not computed in windows having > 1 year of missing data. Spatial synchrony
156 was calculated using the same moving temporal windows by taking the mean of Pearson rank
157 correlations between all pairs of spatial units having > 1 year of missing data during the window.
158 Windows in which < 3 spatial units lacked sufficient data were ignored. We also considered
159 unreliable and discarded EWI statistic measures that were more than than 3.5 standard deviations
160 above or below the mean.

161 Temporal trends in EWI statistics for each species-by-spatial unit combination (temporal CV,
162 lag-1 autocorrelation) or each species (spatial synchrony) were computed using ordinary least
163 squares (OLS) linear regression. Although temporal autocorrelation is a concern for evaluating
164 statistical significance when present, OLS regression provides unbiased estimates of regression
165 parameters even for correlated data, and in this study we did not seek to determine whether trends
166 were statistically significant. To ignore potentially spurious trends supported by few data points,
167 we computed EWI trends only when there were at least 5 EWI measurements spanning no fewer
168 than 10 years. EWI trends were represented by their t -statistic, i.e., the regression parameter
169 describing the linear relationship between the EWI statistic and year divided by its standard error.
170 Thus, we give the largest values to high-magnitude (increasing or decreasing) trends that also
171 have high precision in their estimates (i.e., low variability around the trend). Assigning higher
172 weight to more precisely estimated trends helps to reflect uncertainty that can arise from
173 measurement error or stochasticity. Due to differences in true population size and sampling
174 efficiency, we expected uncertainty to differ among species.

175 We developed an index describing the relative evidence of EWIs for each species by scaling
176 and aggregating the spatial synchrony, temporal CV, and temporal autocorrelation components as
177 follows. As spatial synchrony is already a single value for each species, it was simply rescaled on
178 an interval from 0 (minimum relative risk) to 1 (highest relative risk). Because the temporal CV
179 and temporal autocorrelation components were computed by spatial unit, we first aggregated
180 among spatial units by averaging, and then rescaled to the 0-1 interval. A combined risk index
181 was computed by averaging across the aggregated and rescaled component indices, and again
182 rescaling to the 0-1 interval. Our aggregation and rescaling procedures effectively assign equal
183 weight to all spatial units and component EWI metrics.

184 To investigate whether the EWI score was associated with long-term fish population trends,
185 we examined the Pearson correlation between EWI scores and fish population trends. Fish
186 population trends were quantitatively estimated using mixed effects linear regression with the
187 natural logarithm of CPUE as the response variable, year as a fixed effect, and spatial unit as a
188 random effect on the intercept. Linear mixed effects models were fit using the 'lme4' R package
189 (Bates et al., 2015). To investigate whether the EWI score was associated with native/non-native
190 status, we used analysis of variance in the 'stats' R package (R Core Team, 2024).

191 We also developed an index describing confidence in the relative risk index that takes into
192 account agreement across EWI statistics, invariability among spatial units, and the number of
193 sampling units contributing to the EWI metrics. We assumed that the species for which we could
194 make the most confident assessment were those for which the EWI statistic trends agreed on their
195 sign, for which variability among spatial units in EWI trends is lowest, and for which the EWI
196 estimates were derived from a large number of samples. The confidence score had four
197 components: the base-10 logarithm of total number of sampling events in which a species was
198 detected (i.e., non-zero catch); -1 times the standard deviation (SD) of lag-1 autocorrelation
199 trends (t-values); -1 times the SD of temporal CV trends (t-values), and the number of EWI trends
200 components having the same sign. The SDs of lag-1 autocorrelation trends and temporal CV

201 trends were multiplied by -1 so that larger values would correspond to less variability across
202 spatial units. As above, for the lag-1 autocorrelation trends and the temporal CV trends, t-values
203 for distinct spatial units were averaged to yield one representative metric for each species. Also
204 similar to above, the confidence score components were first rescaled to the 0-1 interval, the
205 components were averaged to produce a combined metric, and this combined metric was again
206 rescaled to the 0-1 interval so that 1 corresponds to the species with the highest confidence score
207 and 0 to the species with the lowest.

208 **Results**

209 Inspection of select EWI time series provides examples in which EWI statistics increased or
210 were elevated corresponding with apparent fish population regime shifts (Figure 2). Delta smelt
211 and striped bass are two species known to have exhibited concerning abundance declines across
212 the study area over recent decades (Moyle et al., 2016; Colombano et al., 2022). Delta smelt, an
213 endangered species, saw its abundances in South the delta confluence region decline substantially,
214 particularly after ≈ 2000 ; over that same period, the lag-1 temporal autocorrelation also increased
215 (Figure 2a). Striped bass, a long-established non-native game fish, was sampled at higher
216 abundances in the delta confluence during the first ≈ 10 years of the time series but was
217 uncommon thereafter; the temporal CV was elevated at the beginning of the time series, declining
218 substantially around the time of population collapse (Figure 2b). Because of a known population
219 collapse in striped bass (Stevens et al., 1985), this pattern was interpreted as being already
220 elevated in the earliest years of our time series because of stability loss and potential regime shifts
221 realized early in the 1980-2023 study period. Mississippi silverside is an invasive forage fish
222 introduced to California in 1967 that has quickly expanded its range (Cook Jr and Moore, 1970;
223 Mahardja et al., 2016); its spatial synchrony rose quickly as population abundances began to
224 increase and has subsequently declined, possibly signaling a transition to a new, high-density
225 population regime (Figure 2c).

226 We focus in the main text on aggregated and relativized metrics, as the central goal of this

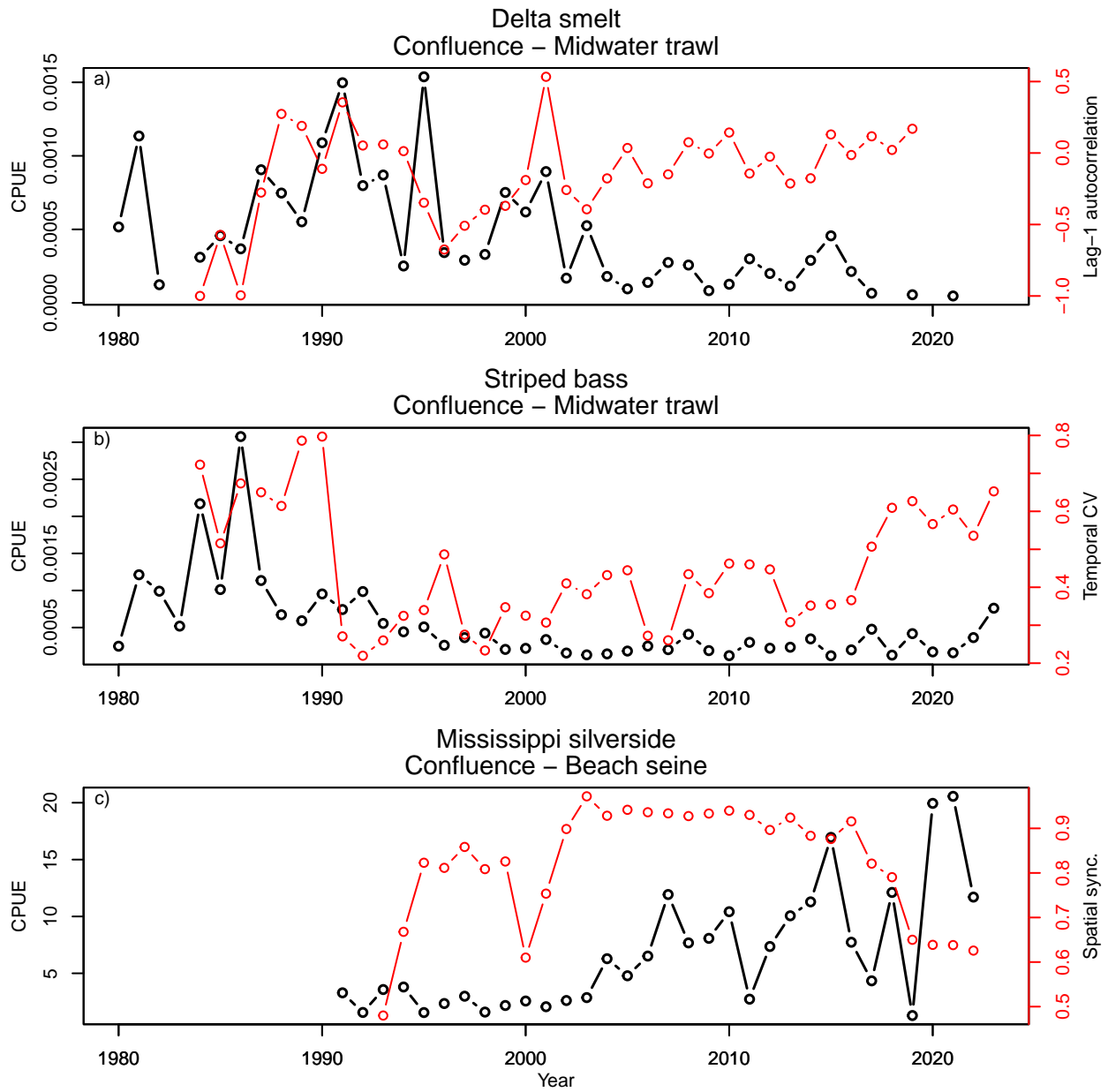


Figure 2: Selected examples of fish population time series (black) and EWI statistics (red). The scale of CPUE differs by sampling method because of different effort measures.

227 study was to develop a relative index of change in EWIs/stability at the species level for our study
228 region; trends in the component metrics for individual species-spatial unit combinations are
229 shown in Supplementary Material Figures S.1-S.3. For context, we provide a brief summary here.
230 The median t-value for trends in temporal CV, across all species and spatial units, was -0.08.
231 After aggregating (averaging) by species, the median t-value was -0.34. The median t-value for
232 trends in lag-1 autocorrelation, across all species and spatial units, was -0.20. After aggregating
233 (averaging) by species, the median t-value was -0.11. The median t-value for trends in spatial
234 synchrony across all species was 1.01; although there was a slight tendency for temporal variance
235 and autocorrelation to have decreased over time, there was a larger-magnitude tendency for
236 spatial synchrony to have increased in more species than it declined.

237 Composite relative EWI scores varied among fishes (Figure 3). Species with the highest EWI
238 scores, corresponding to the greatest loss of population stability compared to the set of studied
239 species, include white croaker, bay pipefish, and tule perch. Species with the lowest risk included
240 northern anchovy, white catfish, and fathead minnow. Species' EWI score components (i.e., EWI
241 metric trend t-statistics, averaged by species and rescaled) were modestly negatively correlated to
242 weakly positively correlated with each other. The Pearson correlation between the spatial
243 synchrony and temporal CV components was -0.04; the Pearson correlation between the trends in
244 spatial synchrony and in lag-1 autocorrelation was 0.32; and the Pearson correlation between the
245 trends in temporal CV and lag-1 autocorrelation was -0.26. EWI scores were uncorrelated with
246 long-term abundance trends (Pearson correlation = 0.11, $p = 0.58$). EWI scores also did not differ
247 between native and non-native species ($F = 0.55$; $df = 1, 27$; $p = 0.47$).

248 Relative confidence also varied substantially among fishes (Figure 4). Fishes with the highest
249 relative confidence included American shad and northern anchovy; fishes with the lowest
250 confidence included bay pipefish, Pacific pompano, and channel catfish.

251 Considering the relative EWI and confidence scores together facilitates categorization of
252 species with, for example, relatively high EWI score and high confidence versus relatively high

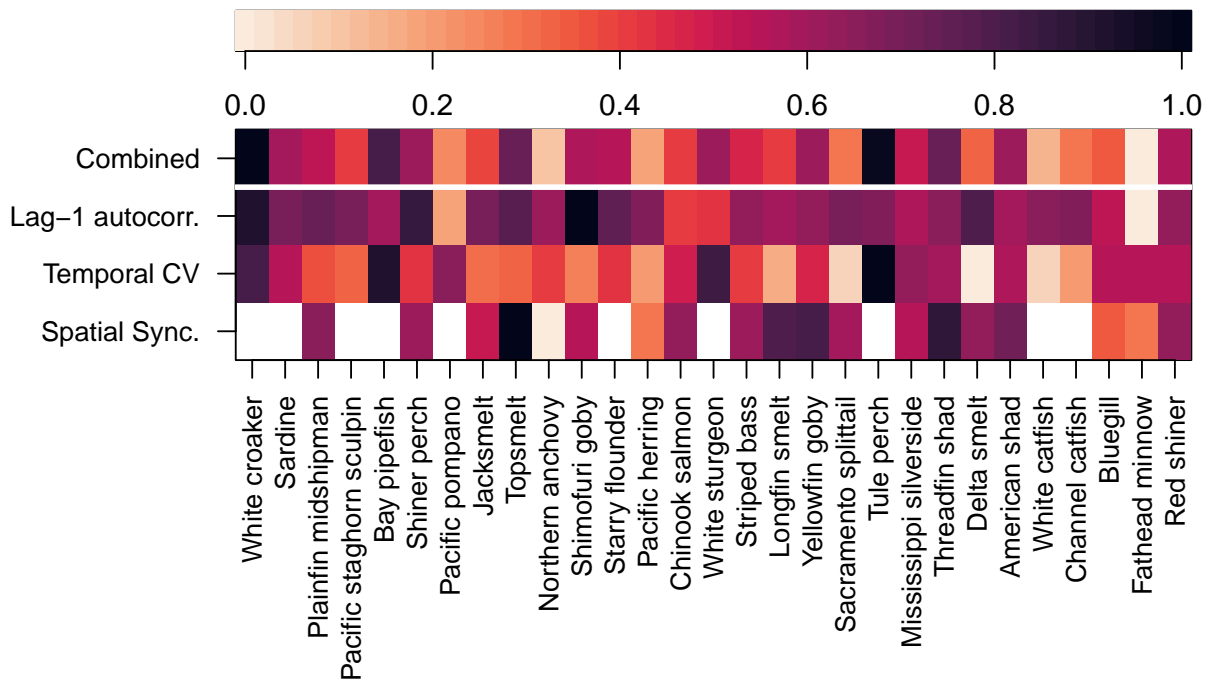


Figure 3: Relative risk of fish population regime shifts based on EWI statistics. The lower 3 rows show relative risk from three component metrics developed by rescaling long-term trends (t-values) to the 0-1 interval. The top row shows the combined (averaged) statistic. Note that several species were not consistently observed in ≥ 3 regions and so the spatial synchrony component was not included.

253 EWI score but low confidence. The species' EWI and confidence scores were not correlated
 254 (Pearson correlation = -0.005, $p = 0.98$).

255 As a robustness check, we also computed results using a window width of 7 years; the EWI
 256 scores and confidence metrics were largely similar regardless of window width (Figures S.4-S.8).
 257 As for the results with a window width of 5 years, the species EWI and confidence scores were
 258 not significantly correlated (Pearson correlation = 0.17, $p = 0.37$). However, there were modest
 259 changes to how species were categorized into quadrants of the EWI score-confidence plot (Figure
 260 S.9). For example, delta smelt, chinook salmon, and striped bass were in quadrant I (high risk,
 261 high confidence) when using a window width of 7 years. These differences were present despite
 262 strong numerical similarities between the scores computed with 5 versus 7 years, highlighting

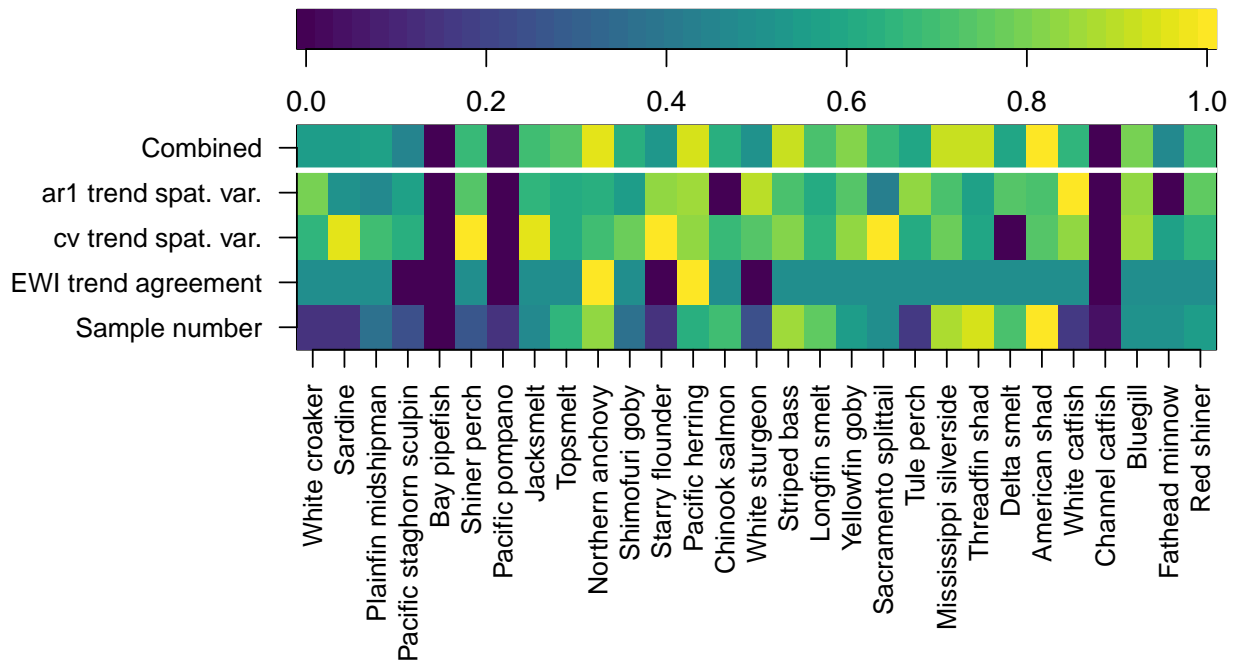


Figure 4: Relative confidence in EWI-based risk assessment. We considered confidence in the EWI score to be highest when the metrics were based on a large number of samples, when the direction of trends in EWI metrics agreed, and when there was less spatial variability in the trends in lag-1 autocorrelation and temporal cv. Note that for the purposes of this metric, the spatial variability in EWI trends have been rescaled so that 1 corresponds to the lowest variability (highest confidence) and 0 corresponds to the greatest variability (lowest confidence).

263 limitations of discrete categorization based on simple thresholds.

264 Discussion

265 Directional trends in metrics of stability that also serve as statistical early warnings of regime
 266 shifts varied widely among fishes in central California, USA, highlighting species exhibiting loss
 267 of stability potentially heralding a nearing regime shift (e.g., white croaker, tule perch, Pacific
 268 lamprey), as well as others that may have gained population stability over the study period (e.g.,
 269 northern anchovy, fathead minnow). Across species, there was no systematic tendency for
 270 temporal variance or autocorrelation to have increased, but spatial synchrony increased on
 271 average. Composite EWI scores, which took into account changes in all three EWI metrics, were
 272 unrelated to long-term population trends or to whether the species is native or non-native. Despite

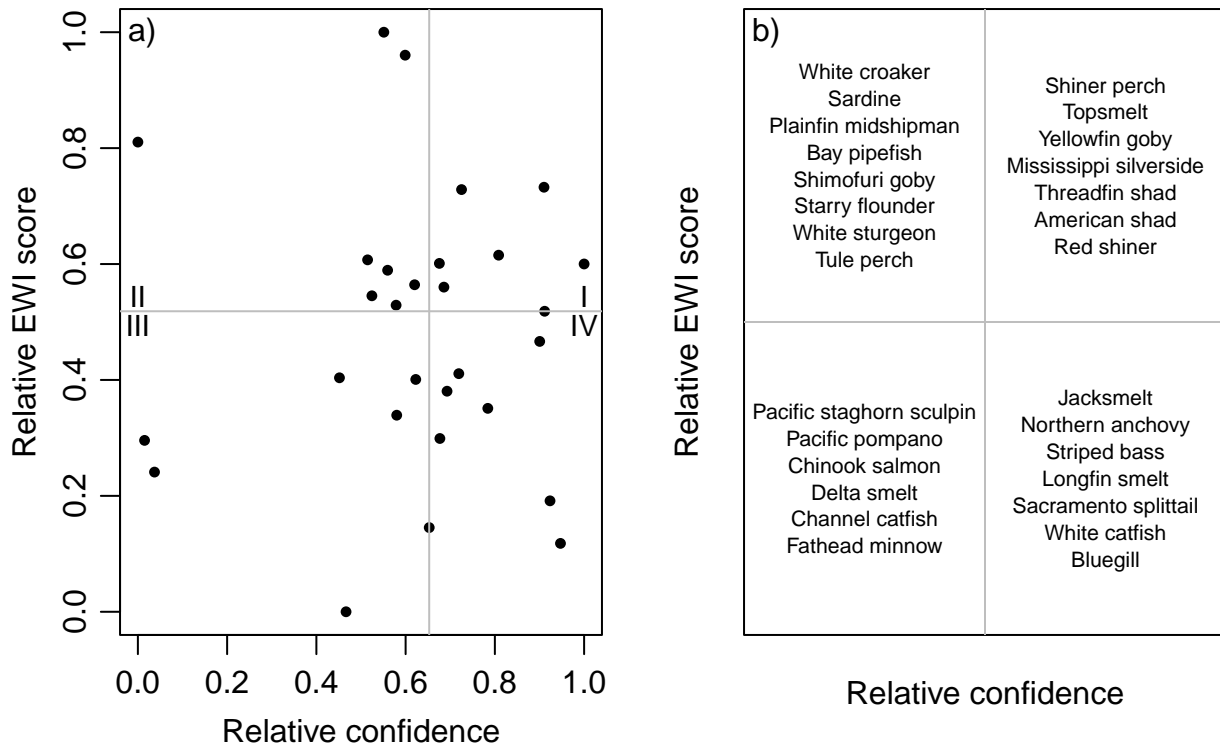


Figure 5: Relative EWI score versus confidence. a) scatterplot of index values; b) names of species in each quadrant of the scatterplot, where quadrant boundaries are defined by the median of each axis.

273 this, the potential for population regime shifts in declining native species like white sturgeon
 274 should be highly concerning for conservation and fishery management, as well as in non-native
 275 species like Mississippi silverside that may transition to a new, high-density regime. Additionally,
 276 the lack of correlation between long-term population trends and EWI scores corroborates that
 277 EWI measures provide information on stability that is largely orthogonal to long-term abundance
 278 trends, as expected. In other words, measures of stability can provide an additional dimension of
 279 information to support decision-making in conservation and natural resource management.

280 In synthesizing across 29 species using data from multiple monitoring programs, we
 281 encountered varying degrees of uncertainty. A primary way we sought to take this into account
 282 was to develop a metric of certainty that took into account agreement across spatial units and EWI
 283 metrics, as well as how more data generally leads to greater precision and a higher signal-to-noise

284 ratio. Simultaneous consideration of the composite EWI scores and the certainty metric can aid
285 decision-making. We propose that the quadrants of Figure 5 can be translated into general
286 recommendations for research and management, though we emphasize that other sources of
287 information should also be used to identify at-risk species and to prioritize research and
288 management efforts. This analysis supports that those in quadrant 1 (high risk, high confidence)
289 be investigated for drivers of population dynamics, to determine whether changes to
290 environmental conditions are having negative consequences, and to ascertain possible population
291 management strategies. Those in quadrant II (high risk, low confidence) should be candidates for
292 additional monitoring to help constrain population variability and temporal dynamics. Those in
293 quadrant III (low risk, low confidence) are also candidates for strengthened monitoring, but may
294 be of lower priority than those in the quadrant II. Those in quadrant IV (low risk, high confidence)
295 would not be prioritized for additional monitoring or research based on these criteria, but may still
296 be high priority based on different criteria.

297 Although we found no systematic association between long-term population trends and the
298 EWI score, we found it notable that four species whose populations have been described as
299 having collapsed (striped bass, Chinook salmon, delta smelt, longfin smelt) had relatively low
300 EWI scores, often with relatively high confidence (Figure 5). While it's not fully known whether
301 the severe and rapid declines of these species precisely fulfill the dynamical assumptions
302 underpinning theory on EWIs, they seem reasonably described as regime shifts in the broad sense.
303 Why, then, in our study have they scored relatively low for evidence of EWIs and loss of stability?
304 A likely explanation is timing: the roots of these population collapses generally began prior to the
305 beginning of our study in 1980 and had already manifest by the middle of the study period. For
306 example, historical surveys suggest that prior to 1980, the first year of this study, delta smelt
307 abundances were markedly higher on average than after (Moyle et al., 2016). In other studies of
308 early warnings of regime shifts, early warning indicators often returned toward normal following
309 the regime shift (Buelo et al., 2018, 2022), so we do not expect EWIs to remain elevated

310 throughout the time series if the population in in a new, low-density regime. Since a primary goal
311 of our approach was to identify species showing current evidence of loss of stability and potential
312 for regime shifts, not to describe regime shifts in the distant past, we consider this characteristic
313 of our results a feature, not a bug. However, this characteristic highlights the importance of
314 temporal frame for understanding ecological trends (Bahlai et al., 2021; Wilkinson et al., 2020).

315 While there was no tendency across species for temporal variance and autocorrelation to have
316 increased through time (i.e., median t-statistics near zero), more than twice as many species
317 exhibited increases in spatial synchrony (13) as decreases (6). In addition to its role as a generic
318 EWI, spatially synchronous metapopulations are thought to be more prone to extinction (Heino
319 et al., 1997), and spatial synchrony is closely related to the stability of total region-wide
320 abundances because the synchronous components of local fluctuations reinforce each other in the
321 regional total, whereas the asynchronous ones tend to cancel out (Anderson et al., 2021). Note
322 that we quantified changes in temporal variance in local spatial units, not in region-wide totals, so
323 these findings are not in conflict. This finding contributes to an emerging consensus that spatial
324 synchrony in biotic variables (e.g., population size, carbon assimilation) has recently risen in
325 many systems, likely as a result of climate change (Reuman et al., 2024; Hansen et al., 2020).

326 Above, we asserted that applying EWIs to annual-interval animal population time series was
327 valuable, particularly considering that change in EWIs corresponds to change in stability even if a
328 tipping point is not near, but that caution was warranted. Selected examples documented change
329 in EWIs that were consistent with apparent regime shifts, such as marked population declines
330 (Figure 2), offering some support. However, rarely did we detect unambiguous increases in the
331 EWIs that were unambiguously *prior to* some apparent state change; the most prominent of these
332 was for Mississippi silverside, where spatial synchrony rose markedly prior to apparent
333 population booms in multiple spatial units (e.g., Figure 2c). Considering this evidence, it seems
334 that EWI metrics may be unable to consistently and reliably provide early warnings when time
335 series are short. Future studies might quantify how time series length and moving window width

336 affect the reliability of EWIs using appropriately realistic simulation models. We remain
337 cautiously optimistic about the value of using generic statistical indicators of stability and regime
338 shifts to animal population time series. They are simple empirical tools that provide information
339 on a dimension of population health beyond long-term trends in mean abundance. While
340 expectations concerning their behavior were first explored through simple theoretical models, the
341 statistics themselves assume little about the dynamics of the underlying system; alternatives like
342 population viability analysis (PVA; Morris and Doak, 2002) make projections that may be more
343 sensitive to underlying model assumptions and structures, though we are not aware of research
344 directly addressing this question. Other methods for reconstructing the stability of empirical
345 (Carpenter et al., 2022) and modeled (Nolting and Abbott, 2016) populations can yield much
346 more detailed and sophisticated insights, but are correspondingly more data hungry and reliant on
347 model assumptions, limiting their potential applications. Approaches like ours could be especially
348 valuable in cases where little is known about organism life history to aid in model design, or when
349 applying a simple and consistent protocol can facilitate comparison across many species.

350 **Acknowledgments**

351 This study was supported by California Department of Fish and Wildlife grant Q2296006.
352 We thank the many researchers and operators who contributed to collection and maintenance of
353 the long-term datasets used in this study.

354 **References**

- 355 Anderson, T. L., L. W. Sheppard, J. A. Walter, R. E. Rolley, and D. C. Reuman. 2021.
356 Synchronous effects produce cycles in deer populations and deer-vehicle collisions. *Ecology*
357 *Letters* **24**:337–347.
- 358 Bahlai, C. A., E. R. White, J. D. Perrone, S. Cusser, and K. S. Whitney. 2021. The broken
359 window: An algorithm for quantifying and characterizing misleading trajectories in ecological
360 processes. *Ecological Informatics* **64**:101336.

361 Bashevkin, S. M., J. W. Gaeta, T. X. Nguyen, L. Mitchell, and S. Khanna, 2024. Fish abundance
362 in the San Francisco Estuary (1959-2024), an integration of 10 monitoring surveys, ver 2. URL
363 <https://doi.org/10.6073/pasta/a29a6e674b0f8797e13fbc4b08b92e5b>.

364 Bates, D., M. Mächler, B. Bolker, and S. Walker. 2015. Fitting Linear Mixed-Effects Models
365 Using lme4. *Journal of Statistical Software* **67**:1–48.

366 Blackburn, S. E., M. L. Gingras, J. DuBois, Z. J. Jackson, and M. C. Quist. 2019. Population
367 dynamics and evaluation of management scenarios for White Sturgeon in the Sacramento–San
368 Joaquin River basin. *North American Journal of Fisheries Management* **39**:896–912.

369 Brown, L. R., W. A. Bennett, R. W. Wagner, T. Morgan-King, N. Knowles, F. Feyrer, D. H.
370 Schoellhamer, M. T. Stacey, and M. Dettinger. 2013. Implications for future survival of delta
371 smelt from four climate change scenarios for the Sacramento–San Joaquin Delta, California.
372 *Estuaries and Coasts* **36**:754–774.

373 Buelo, C., S. Carpenter, and M. Pace. 2018. A modeling analysis of spatial statistical indicators
374 of thresholds for algal blooms. *Limnology and Oceanography Letters* **3**:384–392.

375 Buelo, C., M. Pace, S. Carpenter, E. Stanley, D. Ortiz, and D. Ha. 2022. Evaluating the
376 performance of temporal and spatial early warning statistics of algal blooms. *Ecological*
377 *Applications* **32**:e2616.

378 Carpenter, S. R., M. L. Pace, and G. M. Wilkinson. 2022. DOC, grazers, and resilience of
379 phytoplankton to enrichment. *Limnology and Oceanography Letters* **7**:466–474.

380 Carpenter, S. R., et al. 2011. Early warnings of regime shifts: a whole-ecosystem experiment.
381 *Science* **332**:1079–1082.

382 Colombano, D. D., S. M. Carlson, J. A. Hobbs, and A. Ruhi. 2022. Four decades of climatic
383 fluctuations and fish recruitment stability across a marine-freshwater gradient. *Global change*
384 *biology* **28**:5104–5120.

385 Cook Jr, S., and R. Moore. 1970. Mississippi silversides, *Menidia audens* (Atherinidae),
386 established in California. *Transactions of the American Fisheries Society* **99**:70–73.

387 Dakos, V., S. R. Carpenter, W. A. Brock, A. M. Ellison, V. Guttal, A. R. Ives, S. Kéfi, V. Livina,
388 D. A. Seekell, E. H. van Nes, et al. 2012. Methods for detecting early warnings of critical
389 transitions in time series illustrated using simulated ecological data. *PloS one* **7**:e41010.

390 Dakos, V., M. Scheffer, E. H. Van Nes, V. Brovkin, V. Petoukhov, and H. Held. 2008. Slowing
391 down as an early warning signal for abrupt climate change. *Proceedings of the National*
392 *Academy of Sciences* **105**:14308–14312.

393 Dietze, M. C., A. Fox, L. M. Beck-Johnson, J. L. Betancourt, M. B. Hooten, C. S. Jarnevich, T. H.
394 Keitt, M. A. Kenney, C. M. Laney, L. G. Larsen, et al. 2018. Iterative near-term ecological
395 forecasting: Needs, opportunities, and challenges. *Proceedings of the National Academy of*
396 *Sciences* **115**:1424–1432.

397 Donohue, I., H. Hillebrand, J. M. Montoya, O. L. Petchey, S. L. Pimm, M. S. Fowler, K. Healy,
398 A. L. Jackson, M. Lurgi, D. McClean, et al. 2016. Navigating the complexity of ecological
399 stability. *Ecology letters* **19**:1172–1185.

400 Ellis, S., D. Wainwright, F. Berney, C. Bulman, and N. Bourn. 2011. Landscape-scale
401 conservation in practice: lessons from northern England, UK. *Journal of Insect Conservation*
402 **15**:69–81.

403 Hanak, E. 2011. *Managing California's water: From conflict to reconciliation*. Public Policy
404 Instit. of CA.

405 Hansen, B. B., V. Grøtan, I. Herfindal, and A. M. Lee. 2020. The Moran effect revisited: spatial
406 population synchrony under global warming. *Ecography* **43**:1591–1602.

407 Heino, M., V. Kaitala, E. Ranta, and J. Lindström. 1997. Synchronous dynamics and rates of
408 extinction in spatially structured populations. *Proceedings of the Royal Society of London.*
409 *Series B: biological sciences* **264**:481–486.

410 Kéfi, S., V. Dakos, M. Scheffer, E. H. Van Nes, and M. Rietkerk. 2013. Early warning signals
411 also precede non-catastrophic transitions. *Oikos* **122**:641–648.

412 Kéfi, S., V. Guttal, W. A. Brock, S. R. Carpenter, A. M. Ellison, V. N. Livina, D. A. Seekell,

413 M. Scheffer, E. H. Van Nes, and V. Dakos. 2014. Early warning signals of ecological
414 transitions: methods for spatial patterns. *PloS one* **9**:e92097.

415 Mahardja, B., J. L. Conrad, L. Lusher, and B. Schreier. 2016. Abundance trends, distribution, and
416 habitat associations of the invasive Mississippi Silverside (*Menidia audens*) in the
417 Sacramento–San Joaquin Delta, California, USA. *San Francisco Estuary and Watershed*
418 *Science* **14**.

419 Mandel, J. T., C. J. Donlan, and J. Armstrong. 2010. A derivative approach to endangered species
420 conservation. *Frontiers in Ecology and the Environment* **8**:44–49.

421 Mitchell, L., K. Newman, and R. Baxter. 2017. A covered cod-end and tow-path evaluation of
422 Midwater Trawl gear efficiency for catching Delta Smelt (*Hypomesus transpacificus*). *San*
423 *Francisco Estuary and Watershed Science* **15**.

424 Morris, W. F., and D. D. Doak. 2002. *Quantitative Conservation Biology: Theory and practice of*
425 *population viability analysis*. Sinauer.

426 Moyle, P. B. 2002. *Inland fishes of California: revised and expanded*. Univ of California Press.

427 Moyle, P. B., L. R. Brown, J. R. Durand, and J. A. Hobbs. 2016. Delta smelt: life history and
428 decline of a once-abundant species in the San Francisco Estuary. *San Francisco Estuary and*
429 *Watershed Science* **14**.

430 Moyle, P. B., J. V. Katz, and R. M. Quiñones. 2011. Rapid decline of California’s native inland
431 fishes: a status assessment. *Biological Conservation* **144**:2414–2423.

432 Nolting, B. C., and K. C. Abbott. 2016. Balls, cups, and quasi-potentials: quantifying stability in
433 stochastic systems. *Ecology* **97**:850–864.

434 Pace, M. L., R. D. Batt, C. D. Buelo, S. R. Carpenter, J. J. Cole, J. T. Kurtzweil, and G. M.
435 Wilkinson. 2017. Reversal of a cyanobacterial bloom in response to early warnings.
436 *Proceedings of the National Academy of Sciences* **114**:352–357.

437 Patterson, A. C., A. G. Strang, and K. C. Abbott. 2021. When and where we can expect to see
438 early warning signals in multispecies systems approaching tipping points: insights from theory.

439 The American Naturalist **198**:E12–E26.

440 R Core Team, 2024. R: A Language and Environment for Statistical Computing. R Foundation
441 for Statistical Computing, Vienna, Austria. URL <https://www.R-project.org/>.

442 Reuman, D., J. Walter, L. Sheppard, V. Karatayev, E. Kadiyala, A. Lohmann, T. Anderson,
443 N. Coombs, K. Haynes, L. Hallett, et al. 2024. Insights into spatial synchrony enabled by
444 long-term data. Authorea preprints .

445 Scheffer, M., J. Bascompte, W. A. Brock, V. Brovkin, S. R. Carpenter, V. Dakos, H. Held, E. H.
446 Van Nes, M. Rietkerk, and G. Sugihara. 2009. Early-warning signals for critical transitions.
447 Nature **461**:53–59.

448 Schindler, D. E., J. B. Armstrong, and T. E. Reed. 2015. The portfolio concept in ecology and
449 evolution. *Frontiers in Ecology and the Environment* **13**:257–263.

450 Seekell, D. A., S. R. Carpenter, and M. L. Pace. 2011. Conditional heteroscedasticity as a leading
451 indicator of ecological regime shifts. *The American Naturalist* **178**:442–451.

452 Stevens, D. E., D. W. Kohlhorst, L. W. Miller, and D. Kelley. 1985. The decline of striped bass in
453 the Sacramento-San Joaquin Estuary, California. *Transactions of the American Fisheries*
454 *Society* **114**:12–30.

455 Stompe, D. K., P. B. Moyle, A. Kruger, and J. R. Durand. 2020. Comparing and integrating fish
456 surveys in the San Francisco Estuary: why diverse long-term monitoring programs are
457 important. *San Francisco Estuary and Watershed Science* **18**.

458 Tempel, T. L., T. D. Malinich, J. Burns, A. Barros, C. E. Burdi, and J. A. Hobbs. 2021. The value
459 of long-term monitoring of the San Francisco Estuary for delta smelt and longfin smelt. *Calif*
460 *Fish Game* **107**:148–171.

461 Tobias, V. D., E. Chen, J. Hobbs, M. Eakin, and S. Detwiler. 2023. Informing extinction risk:
462 Summarizing population viability through a meta-analysis of multiple long-term monitoring
463 programs for a declining estuarine fish species. *Biological Conservation* **288**:110348.

464 Wang, S., and M. Loreau. 2014. Ecosystem stability in space: α , β and γ variability. *Ecology*

465 letters **17**:891–901.

466 Wilkinson, G. M., S. R. Carpenter, J. J. Cole, M. L. Pace, R. D. Batt, C. D. Buelo, and J. T.
467 Kurtzweil. 2018. Early warning signals precede cyanobacterial blooms in multiple whole-lake
468 experiments. *Ecological Monographs* **88**:188–203.

469 Wilkinson, G. M., J. Walter, R. Fleck, and M. L. Pace. 2020. Beyond the trends: The need to
470 understand multiannual dynamics in aquatic ecosystems. *Limnology and Oceanography*
471 *Letters* **5**:281–286.

472 Willis, A. D., R. A. Peek, and A. L. Rypel. 2021. Classifying California’s stream thermal regimes
473 for cold-water conservation. *PLoS One* **16**:e0256286.

474 Yarnell, S. M., G. E. Petts, J. C. Schmidt, A. A. Whipple, E. E. Beller, C. N. Dahm, P. Goodwin,
475 and J. H. Viers. 2015. Functional flows in modified riverscapes: hydrographs, habitats and
476 opportunities. *BioScience* **65**:963–972.

477 Zale, A. V., D. L. Parrish, and T. M. Sutton. 2012. *Fisheries techniques*. American Fisheries
478 Society Bethesda, Maryland.

Supplementary Information to: Quantifying changes in fish population stability using statistical early warnings of regime shifts

Jonathan A. Walter¹, Levi S. Lewis², James A. Hobbs², and Andrew L. Rypel^{1,2}

¹Center for Watershed Sciences, University of California, Davis, California, USA

²Department of Wildlife, Fish, and Conservation Biology, University of California, Davis, California, USA

Contact: jawalter@ucdavis.edu

Species	Habitat	Family	Native
White croaker <i>Genyonemus lineatus</i>	Marine, Benthopelagic	Sciaenidae	Yes
Sardine <i>Sardinops sagax</i>	Marine, Pelagic	Alosidae	Yes
Plainfin midshipman <i>Porichthys notatus</i>	Marine, brackish, Demersal	Batrachoididae	Yes
Pacific staghorn sculpin <i>Leptocottus armatus</i>	Marine, brackish Demersal	Cottidae	Yes
Bay pipefish <i>Syngnathus leptorhynchus</i>	Marine, brackish, Demersal	Syngnathidae	Yes
Shiner perch <i>Cymatogaster aggregata</i>	Marine, brackish Benthopelagic	Embiotocidae	Yes
Pacific pompano <i>Peprilus simillimus</i>	Marine, brackish Benthopelagic	Stromateidae	Yes
Jacksmelt <i>Atherinopsis californiensis</i>	Marine, brackish Pelagic	Atherinopsidae	Yes
Topsmelt <i>Atherinops affinis</i>	Marine, brackish, Pelagic	Atherinopsidae	Yes
Northern anchovy <i>Engraulis mordax</i>	Marine, brackish Pelagic	Engraulidae	Yes
Shimofuri goby <i>Tridentiger bifasciatus</i>	Marine, brackish, Demersal	Oxudercidae	No
Starry flounder <i>Platilichthys stellatus</i>	Marine, brackish, fresh, Demersal	Pleuronectidae	Yes

Pacific herring <i>Clupea pallasii</i>	Marine, brackish Benthopelagic	Clupeidae	Yes
Chinook salmon <i>Oncorhynchus tshawytscha</i>	Marine, brackish, fresh, Benthopelagic	Salmonidae	Yes
White sturgeon <i>Acipenser transmontanus</i>	Marine, brackish, fresh, Demersal	Acipenseridae	Yes
Striped bass <i>Morone saxatilis</i>	Marine, brackish, fresh, Benthopelagic	Moronidae	No
Longfin smelt <i>Spirinchus thaleichthys</i>	Marine, brackish, fresh Benthopelagic	Osmeridae	Yes
Yellowfin goby <i>Acanthogobius flavimanus</i>	Brackish, Demersal	Oxudercidae	No
Sacramento splittail <i>Pogonichthys macrolepidotus</i>	Brackish, freshwater, Benthopelagic	Cyprinidae	Yes
Tule perch <i>Hysterocarpus traskii</i>	Brackish, freshwater, Benthopelagic	Embiotocidae	Yes
Mississippi silverside <i>Menidia audens</i>	Brackish, fresh, Pelagic	Atherinidae	No
Threadfin shad <i>Dorosoma petenense</i>	Brackish, freshwater, Pelagic	Dorosomatidae	No
Delta smelt <i>Hypomesus transpacificus</i>	Brackish, freshwater, Pelagic	Osmeridae	Yes
American shad <i>Alosa sapidissima</i>	Brackish, freshwater, Pelagic	Alosidae	No
White catfish <i>Ameiurus catus</i>	Freshwater Demersal	Ictaluridae	No
Channel catfish <i>Ictalurus punctatus</i>	Freshwater, Demersal	Ictaluridae	No
Bluegill <i>Lepomis macrochirus</i>	Freshwater, Benthopelagic	Centarchidae	No
Fathead minnow <i>Pimephales promelas</i>	Freshwater, Demersal	Cyprinidae	No
Red shiner <i>Cyprinella lutrensis</i>	Freshwater, Benthopelagic	Cyprinidae	No

Table S.1: Attributes of fish species used in this study. Information is from Fishbase and expert knowledge.

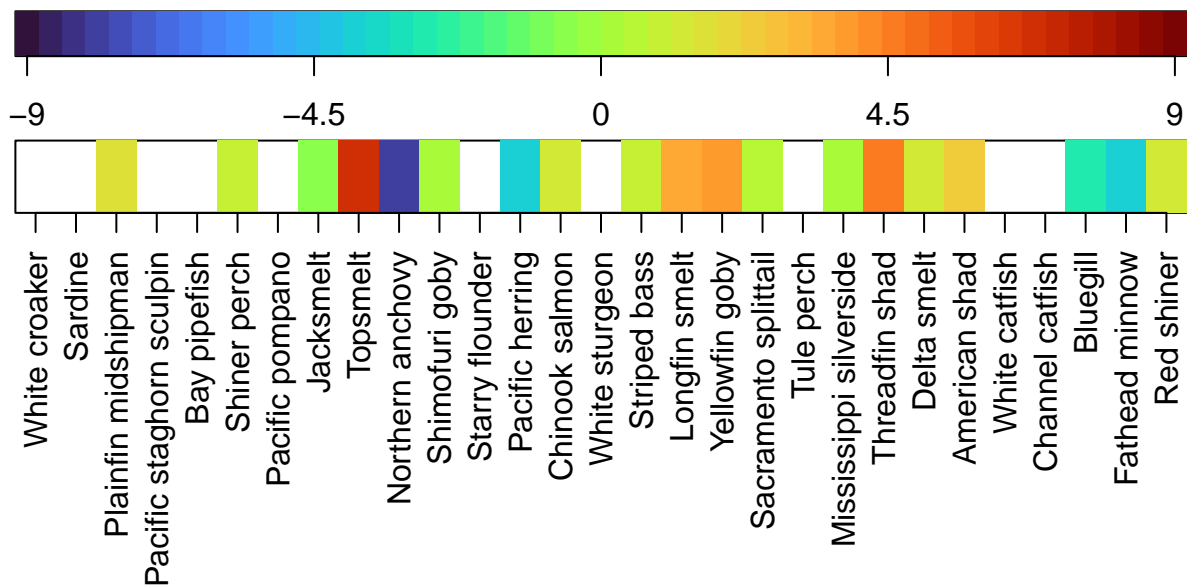


Figure S.1: Temporal trends (t-values) in spatial synchrony of fall age-0 CPUE by species. Blank cells indicate that insufficient data were available to compute the trend in spatial CV, e.g., because the species was not consistently caught by multiple region-gear type combinations.

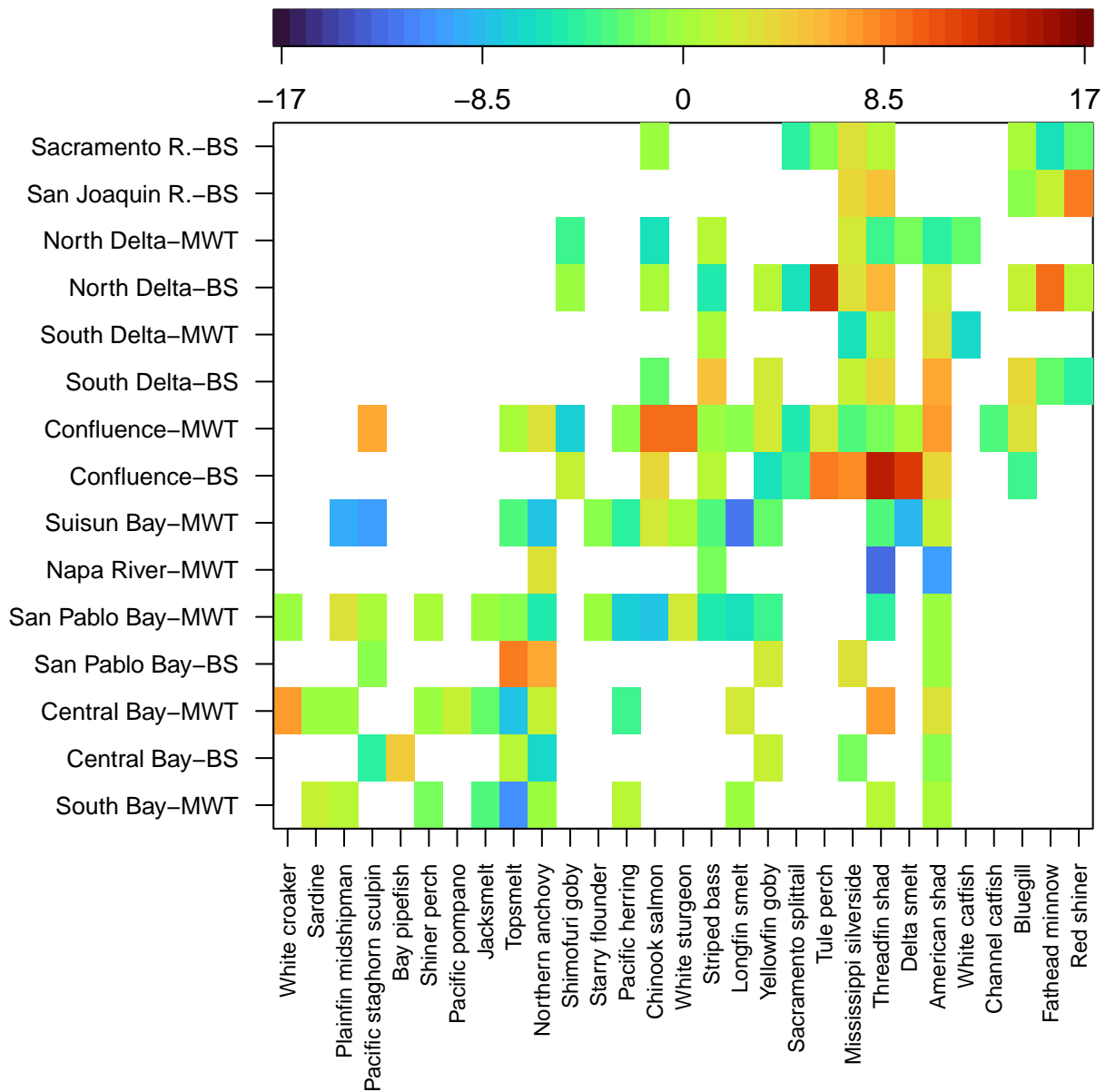


Figure S.2: Temporal trends (t-values) in the temporal coefficient of variation (CV) of fall age-0 CPUE by species and region-gear type combination. Blank cells indicate that insufficient data were available to compute the trend in temporal CV.

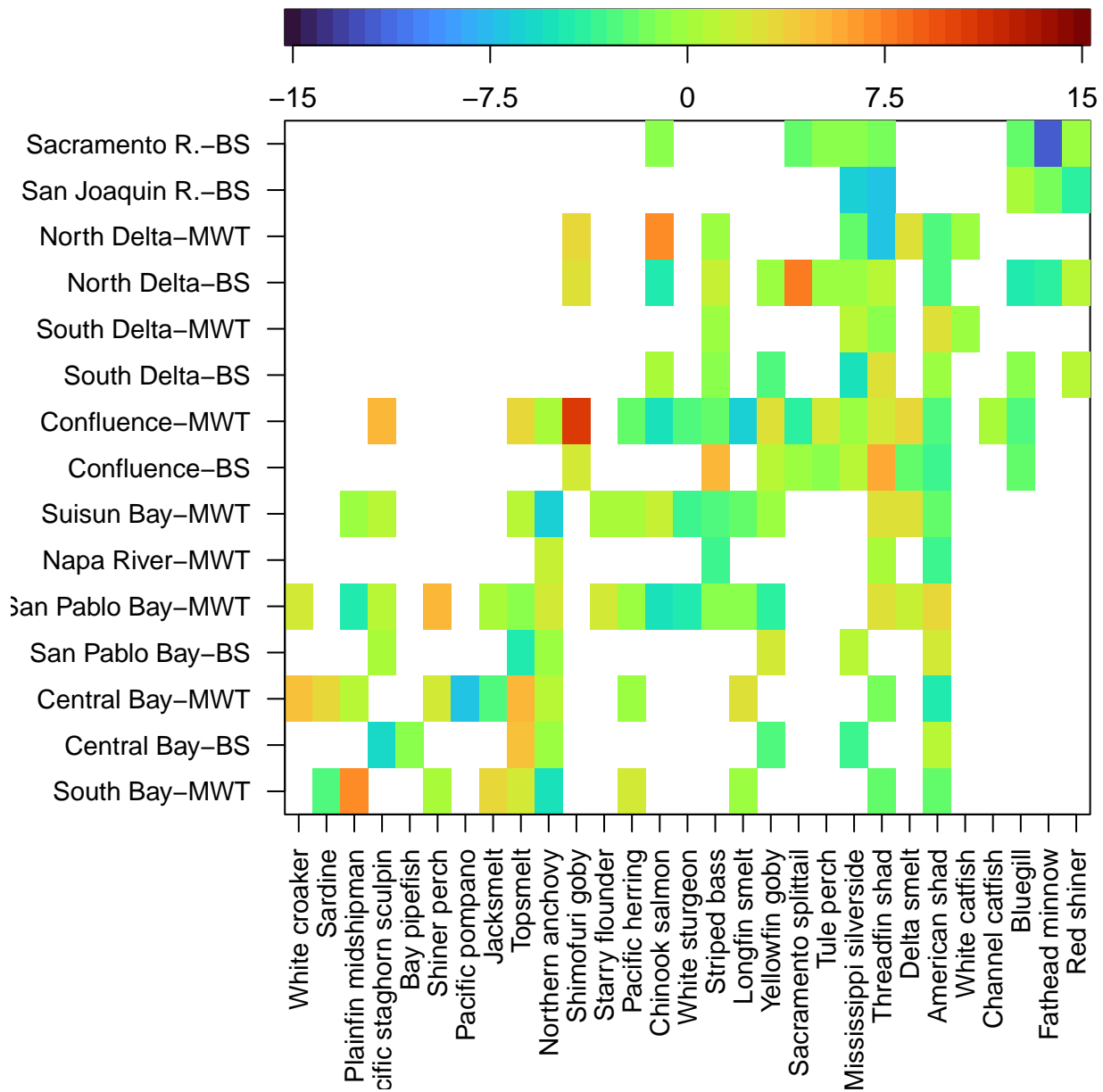


Figure S.3: Temporal trends (t-values) in the lag-1 temporal autocorrelation of fall age-0 CPUE by species and region-gear type combination. Blank cells indicate that insufficient data were available to compute the trend in lag-1 autocorrelation.

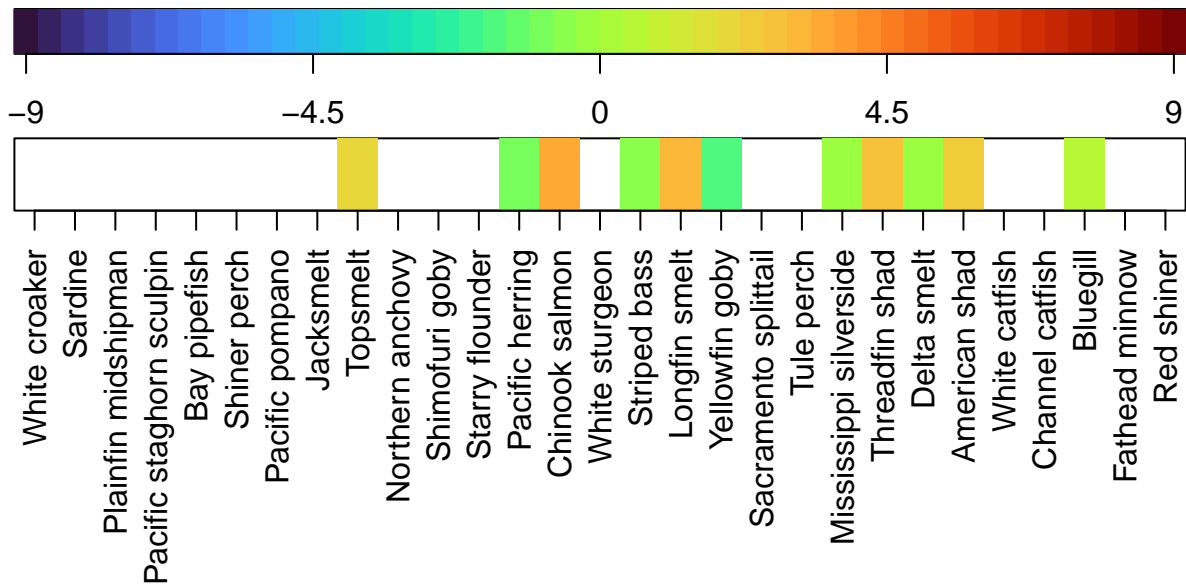


Figure S.4: Temporal trends (t-values) in spatial synchrony of fall age-0 CPUE by species using a 7-year window width. Blank cells indicate that insufficient data were available to compute the trend in spatial CV, e.g., because the species was not consistently caught by multiple region-gear type combinations.

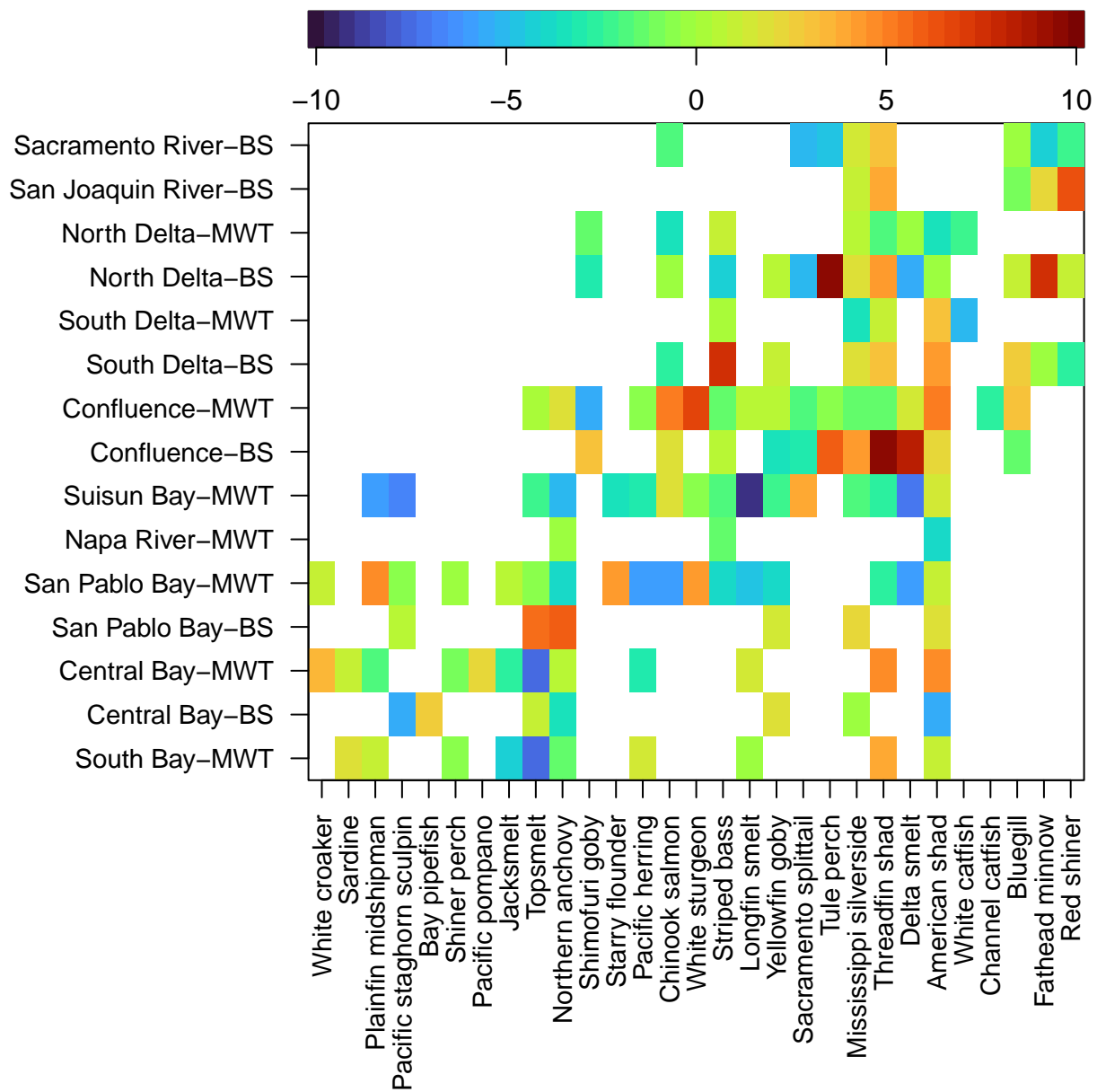


Figure S.5: Temporal trends (t-values) in the temporal coefficient of variation (CV) of fall age-0 CPUE by species and region-gear type combination using a 7-year window width. Blank cells indicate that insufficient data were available to compute the trend in temporal CV.

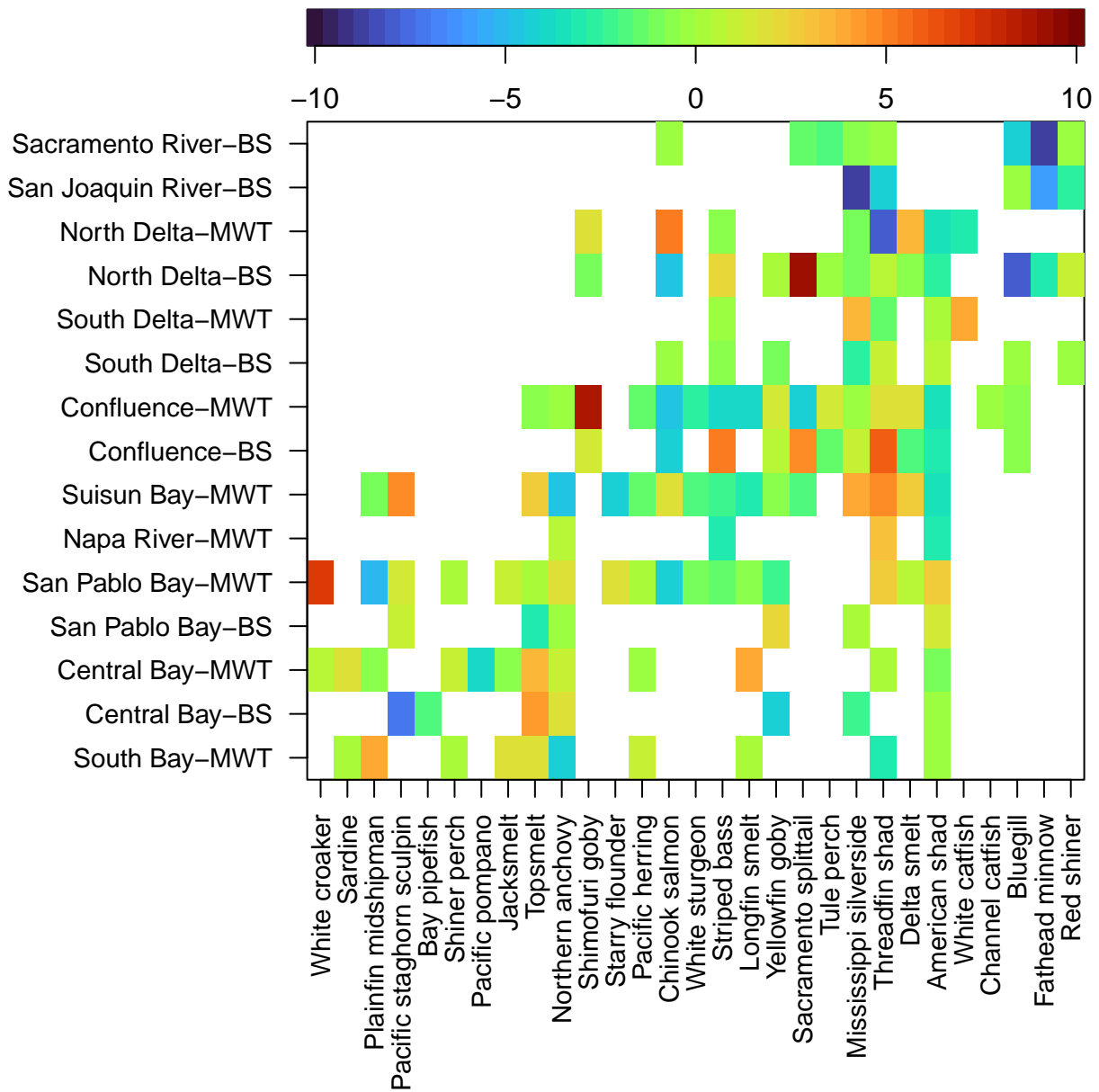


Figure S.6: Temporal trends (t-values) in the lag-1 temporal autocorrelation of fall age-0 CPUE by species and region-gear type combination using a 7-year window width. Blank cells indicate that insufficient data were available to compute the trend in lag-1 autocorrelation.

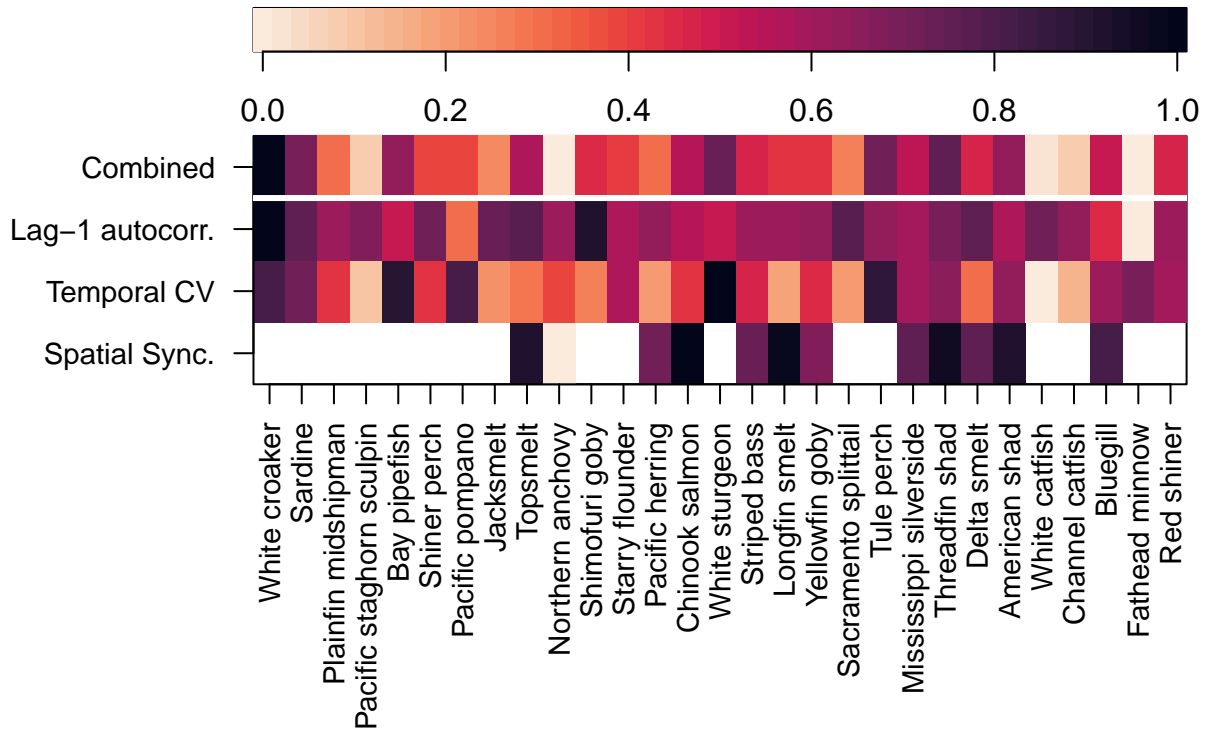


Figure S.7: Relative risk of fish population regime shifts based on EWI statistics using a window width of 7 years. The lower 3 rows show relative risk from three component metrics developed by rescaling long-term trends (t-values) to the 0-1 interval. The top row shows the combined (averaged) statistic. Note that several species were not consistently observed in ≥ 3 regions and so the spatial synchrony component was not included.

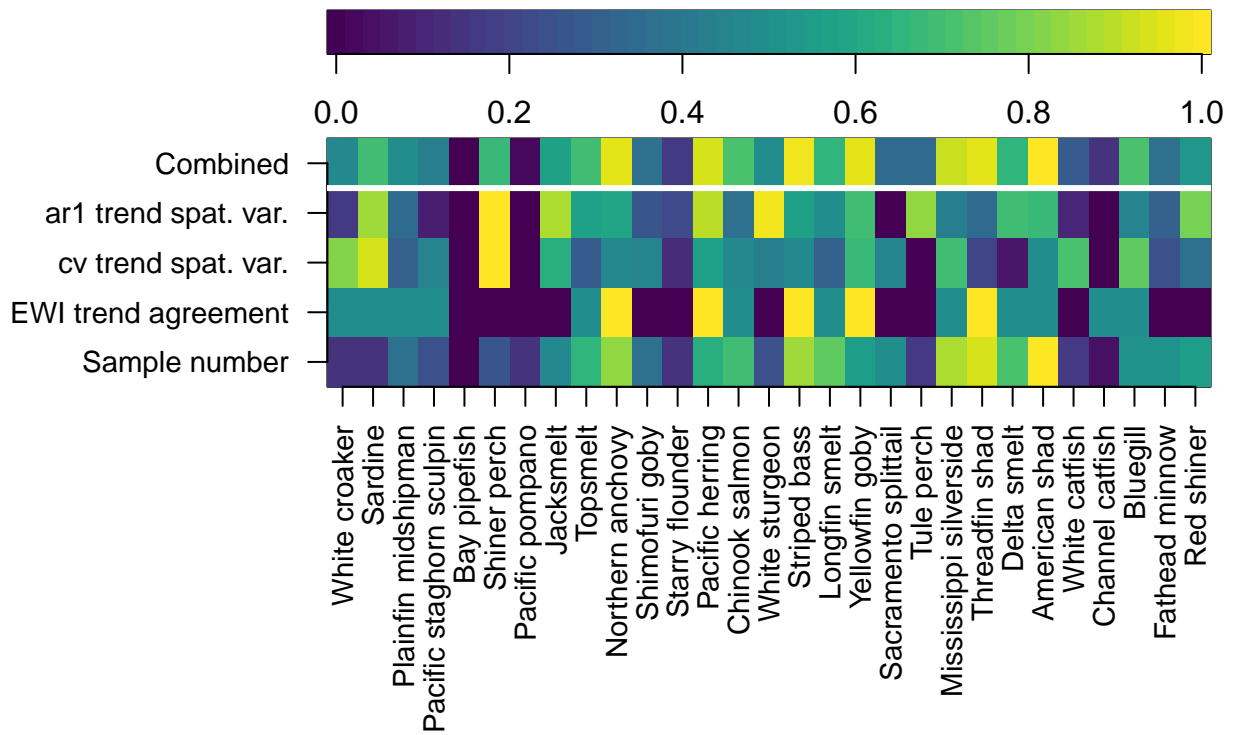


Figure S.8: Relative confidence in EWI-based risk assessment using a 7-year window width. We considered confidence in the EWI score to be highest when the metrics were based on a large number of samples, when the direction of trends in EWI metrics agreed, and when there was less spatial variability in the trends in lag-1 autocorrelation and temporal cv. Note that for the purposes of this metric, the spatial variability in EWI trends have been rescaled so that 1 corresponds to the lowest variability (highest confidence) and 0 corresponds to the greatest variability (lowest confidence).

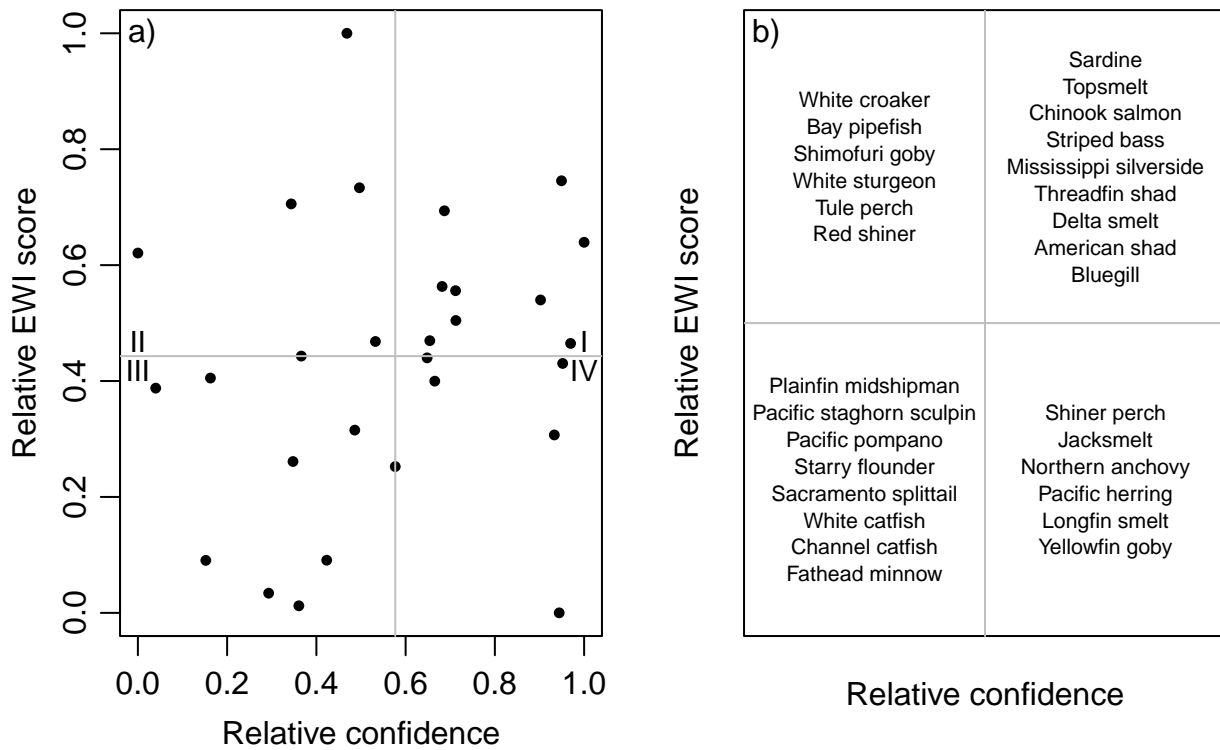


Figure S.9: Relative EWI score versus confidence using a 7-year window width. a) scatterplot of index values; b) names of species in each quadrant of the scatterplot, where quadrant boundaries are defined by the median of each axis.